Inorganic Chemistry
Cite This: Inorg. Chem. 2018, 57, 2973−2976
Communication
pubs.acs.org/IC

Unusual Coexistence of Nickel(II) and Nickel(IV) in the Quadruple Perovskite $Ba_4Ni_2Ir_2O_{12}$ Containing Ir_2NiO_{12} Mixed-Metal-Cation Trimers

Timothy Ferreira,[†] Steve M. Heald,[‡] Mark. D. Smith,[†] and Hans-Conrad zur Loye*[,†]

[†]Department of Chemistry and Biochemistry, University of South Carolina, Columbia, South Carolina 29208, United States
[‡]X-ray Science Division, Advanced Photon Source (APS), Argonne National Laboratory (ANL), Argonne, Illinois 60439, United States

Supporting Information

ABSTRACT: The crystal chemistry and magnetic properties of two hexagonal nickel(IV)-containing perovskites, $Ba_4Ni_{1.94}Ir_{2.06}O_{12}$ and $BaNiO_3$, are reported. The 12R perovskite, $Ba_4Ni_{1.94}Ir_{2.06}O_{12}$, possesses an unexpected coexistence of nickel(II) and nickel(IV). This quadruple perovskite structure contains Ir_2NiO_{12} mixed-metal-cation units in which direct metal−metal bonding between nickel(IV) and iridium(V) is inferred. X-ray absorption near-edge spectroscopy and X-ray photoelectron spectroscopy measurements were conducted to confirm the simultaneous presence of nickel(II) and nickel(IV).

Iridium-containing oxides have attracted significant interest as model systems in which to study unusual electronic and magnetic ground states that can lead to properties such as superconductivity,[1] topological insulation,[2] and spin-liquid states.[3] Complex iridates serve as a playground for studying how small changes in the chemical environment can affect the electronic structure because of iridium's typical strong spin−orbit coupling that competes with crystal-field effects from the surrounding oxygen.[4−9] In addition to these competing interactions, the large orbital extent and high valence attainable in the heavy 5d elements are responsible for the possibility of direct metal−metal bonding in iridium-containing solid-state materials and the associated changes to the electronic structures.[10−14] For these and other reasons, iridium-containing oxides, including complex perovskites, continue to be of interest.

The perovskite structure ABO_3 is quite versatile and, in oxides, can accommodate various ratios of A:B and B:B′ cations by forming double $A_2BB'O_6$ (B ≠ B′), triple $A_3BB'_2O_9$, and hexagonal quadruple $A_4BB'_3O_{12}$ perovskites.[15] Within this diverse structural assortment, numerous nickel-containing perovskites are known, where typically nickel is present in the 2+ oxidation state, such as in $Sr_2Ni_2OsO_6$[16] and Sr_2NiWO_6;[17] however, nickel can adopt higher oxidation states in perovskites, such as 3+ in $LaNiO_3$ and 4+ in $BaNiO_3$. Similarly, iridium is well represented in perovskites in a number of oxidation states, including 4+, 5+, and 6+ in double, triple, and quadruple perovskites.[12,13,18−23]

A significant number of quadruple perovskites containing iridium of the type $Ba_4BIr_3O_{12}$ have been prepared and studied for their magnetic behavior, which is often dominated by the Ir_3O_{12} trimer unit.[12,13] Quadruple perovskites of the type $Ba_4B_2Ir_2O_{12}$, containing a Ir_2BO_{12} trimer (B ≠ Ir), have not been reported to date. One reason for this absence is that it is rare to have a B:B′ ratio of 2:2 that forms a quadruple hexagonal instead of a cubic or distorted double perovskite. One condition that would favor the formation of a quadruple perovskite instead is the presence of mixed-valent B cations. Mixed valency in perovskites is not unknown; however, unless a charge disproportionation takes place, where one of the cations is present in a significantly different oxidation state from the other, it is unlikely for them to charge-order in the structure.[24] Herein we communicate the synthesis and crystal structure of a new 12R quadruple perovskite, $Ba_4Ni_{1.94}Ir_{2.06}O_{12}$, that possesses an unexpected coexistence of $Ni^{II}O_6$ and $Ni^{IV}O_6$ units that for size reasons lead to structural ordering and that allow for the formation of the unusual Ir_2NiO_{12} trimer.

Phase-pure single crystals of $Ba_4Ni_{1.94}Ir_{2.06}O_{12}$ were synthesized via a wet hydroxide flux growth using 1.5 mmol of $Ba(OH)_2{\cdot}8H_2O$ (Alfa Aesar; 98+%), 0.33 mmol of NiO (Alfa Aesar; 99%), 1.0 mmol of iridium metal (Engelhard; 99.9995%), 5.0 g of KOH (BDH; ACS grade), and 1.0 mL of distilled water contained in a sealed silver tube. The reaction was heated to 700 °C at a ramp rate of 600 °C/h, held for 24 h, and cooled to 300 °C at a rate of 6 °C/h. The flux was dissolved in water, and the crystals were isolated by vacuum filtration. Phase-pure single crystals of $BaNiO_3$ were synthesized and isolated in the same way as $Ba_4Ni_{1.94}Ir_{2.06}O_{12}$, with the exception of an increased dwell temperature of 750 °C and the absence of iridium metal as a reagent. See the Supporting Information for details on the experimental setup of single-crystal structural determination, X-ray absorption near-edge spectroscopy (XANES), and SQUID measurements.

In order to confirm the oxidation states of the first-row cations, XANES and X-ray photoelectron spectroscopy (XPS) were performed. The hexagonal perovskite $BaNiO_3$, which contains nickel(IV) in a chemical environment similar to that of nickel(IV) in $Ba_4Ni_{1.94}Ir_{2.06}O_{12}$, was also synthesized for comparative purposes, both as an appropriate model for the rare $Ni^{IV}O_6$ coordination environment and as a reference for the magnetism of nickel(IV) in an oxide environment. The presence of the different nickel oxidation states in $Ba_4Ni_{1.94}Ir_{2.06}O_{12}$,

Received: January 31, 2018
Published: March 2, 2018

DOI: 10.1021/acs.inorgchem.8b00249
Inorg. Chem. 2018, 57, 2973−2976

combined with the presence of mixed cation Ir_2NiO_{12} units, results in an overall magnetic moment that can be explained by invoking the presence of direct metal−metal bonding between iridium(V) and nickel(IV).

The 12R quadruple perovskite structure contains B'_3O_{12} units consisting of three face-sharing octahedra; these units are connected to each other via corner-sharing BO_6 octahedra, as shown in Figure 1. By comparison, the structurally related 2H

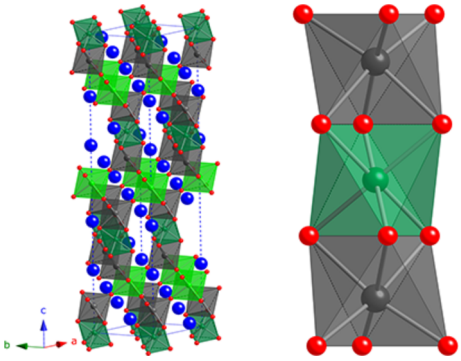

Figure 1. (Left) Polyhedral representation of $Ba_4Ni_{1.94}Ir_{2.06}O_{12}$ with nickel(II) shown in light green, nickel(IV) shown in dark green, iridium(V) shown in gray, barium shown in blue, and oxygen shown in red. (Right) Local coordination environment of nickel(IV) octahedra, shown in dark green, face-shared with two distorted iridium(V) octahedra, shown in gray.

hexagonal perovskite $BaNiO_3$ contains infinite chains of face-sharing octahedra, as shown in Figure S1, with crystallographic information for both structures found in Table S1. A scanning electron microscopy (SEM) image of representative single crystals of both compositions is shown in Figure S2.

Unlike generic 12R quadruple perovskites, $A_4BB'_3O_{12}$, which have two crystallographically unique sites with one metal on each site (BO_6 octahedra and B'_3O_{12} trimers: $B \neq B'$), the mixed valence of nickel(II) and nickel(IV) "forces" nickel to be present on both sites for size reasons. This results in $Ni^{II}O_6$ octahedra in addition to mixed Ir_2NiO_{12} units, which contain both nickel(IV) and iridium(V) (Figures 1 and S3). To assess the nickel oxidation states, bond-valence-sum (BVS) calculations were carried out on both NiO_6 and IrO_6 octahedral environments, as shown in Table S2. The six Ni−O bonds in the corner-shared octahedra, which bridge the Ir_2NiO_{12} trimers, are 2.056(3) Å, corresponding to a BVS value of 2.05, indicating nickel(II). The six Ni−O bonds in the Ir_2NiO_{12} trimers are 1.925(3) Å, corresponding to a BVS value of 3.95, indicating nickel(IV). The iridium cations have three long [2.020(3) Å] and three short [1.952(3) Å] bonds each, resulting in a BVS sum of 5.12, indicating iridium(V).

This result was corroborated by XANES measurements performed at Beamline 20-BM at the APS at ANL, as shown in Figure 2. Higher binding energies are expected for higher oxidation states, and thus three nickel-containing compounds ranging from zero valent to tetravalent nickel were measured for reference, in addition to the title compound. The binding energies for all measured compounds are included in Table S3. The observed binding energy for $Ba_4Ni_{1.94}Ir_{2.06}O_{12}$ is 1 eV lower than that of $BaNi(IV)O_3$, consistent with the presence of both nickel(II) and nickel(IV) in the title compound. The binding energy of $Ba_4Ni_{1.94}Ir_{2.06}O_{12}$ is 1 eV higher than that of $Ni^{II}O$, as expected for a mixed nickel(IV/II)-containing compound, thus supporting the BVS findings. XANES measurements (Table S4

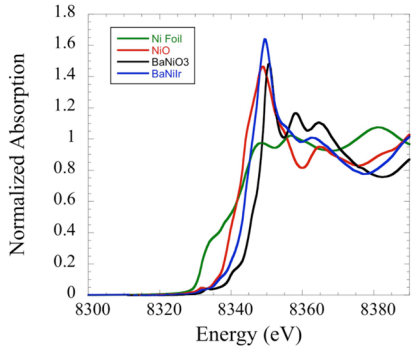

Figure 2. XANES measurement of binding energies plotted against normalized absorption for metallic nickel metal, NiO, $BaNiO_3$, and $Ba_4Ni_{1.94}Ir_{2.06}O_{12}$.

and Figure S4) comparing the title compound to IrO_2 confirmed the presence of iridium(V). XPS measurements were conducted and are consistent with the presence of nickel(IV) (Figure S5 and Table S5).

The simultaneous presence and charge ordering of nickel(II) and nickel(IV) is unexpected, but one might suspect that the presence of Ir_2NiO_{12} mixed-metal-cation units stabilize nickel(IV) in the presence of nickel(II). It also suggests that the iridium cations strongly favor 5+ over 4+ oxidation state under the synthetic conditions used because otherwise a $Ba_2Ni^{IV}Ir^{IV}O_6$ double perovskite would potentially have formed. The formation of the titled composition over the possible double perovskite is supported by the Goldschmidt tolerance factor for the theoretical double perovskite of $t = 1.027$, indicating that a hexagonal phase is favored over a cubic one.[25]

A plot of the temperature dependence of the field-cooled (FC) and zero-field-cooled (ZFC) magnetic susceptibility data collected at 0.1 T is shown in Figure 3, with a clean powder X-

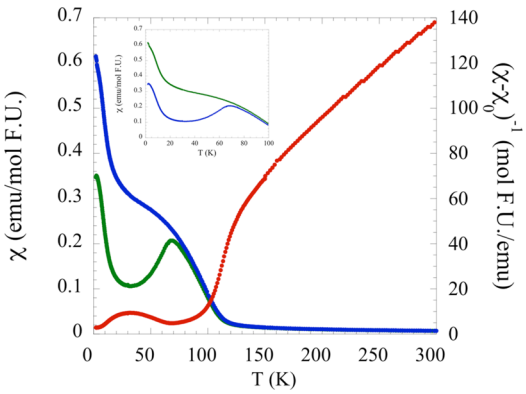

Figure 3. Temperature dependence of the magnetic susceptibility for $Ba_4Ni_{1.94}Ir_{2.06}O_{12}$ at 0.1 T, with FC data shown in blue, ZFC data shown in green, and the inverse magnetic susceptibility shown in red.

ray diffraction (PXRD) confirming the accuracy of these results, as shown in Figure S6. Significant field dependence and multiple magnetic transitions are observed, with the highest being at 115 K. Although the negative Weiss temperature ($\theta_{cw} = -33$ K) is indicative of antiferromagnetic interactions, a number of ferromagnetic-like interactions are observed at $T = 30$ and 115 K, likely indicating competing ferromagnetic and antiferromagnetic interactions. This ferromagnetic-like behavior is further observed in Figures S7−S10. The presence of hysteresis at 2 and 45 K is indicative of possible ferrimagnetic order or spin canting.

DOI: 10.1021/acs.inorgchem.8b00249
Inorg. Chem. 2018, 57, 2973−2976

The $\chi_M T$ versus T plots at both 0.1 and 1 T indicate ferromagnetic-like interactions, corroborating possible ferrimagnetic order. It should be noted, however, that, in the absence of magnetic neutron diffraction investigations, an unambiguous assignment of the magnetic order cannot be made.

When the high-temperature paramagnetic regime of the 1 T magnetic susceptibility data of $Ba_4Ni_{1.94}Ir_{2.06}O_{12}$ is fit to the Curie–Weiss law, with a χ_0 term, as shown in Figure S11, an effective magnetic moment of 4.40 μ_B is obtained. Given that in $Ba_4Ni_{1.94}Ir_{2.06}O_{12}$ nickel(II) has two unpaired electrons, that nickel(IV) has a low-spin t_{2g}^6 electron configuration, and that iridium(V) adopts a nonmagnetic ground state[5,7−9,26,27] due to spin orbit coupling, as shown in Figure S12, we would expect a calculated spin-only moment of 2.83 μ_B. This value is significantly lower than the measured value of 4.40 μ_B. To confirm that nickel(IV) in an octahedral coordination environment is nonmagnetic, unlike recent reports of ferromagnetic nickel(IV) in the cubic perovskite $SrFe_{0.6}Ni_{0.4}O_3$,[28] we collected magnetic susceptibility data for $BaNiO_3$ (Figure S13), confirming the expected diamagnetic result for $Ni^{IV}O_6$.

To rationalize the measured magnetic moment of 4.40 μ_B, we need to treat the nickel(IV) and two iridium(V) cations as an independent Ir_2NiO_{12} trimeric unit. The description of nickel(IV) and iridium(V) behaving as one Ir_2NiO_{12} can be understood as resulting from direct metal–metal bonding, leading to a new electronic structure. The short distance between the iridium(V) and nickel(IV) [2.562(3) Å] makes direct metal–metal bonding probable. The resultant electronic structure can be estimated using the previously reported schematic energy-level diagrams published to model the 14-electron $Ir_3^{4.33+}O_{12}$ trimers in the quadruple perovskite $Ba_4LnIr_3O_{12}$ (Ln = La, Nd–Gd, Dy–Lu).[13] Using the local D_{3d} symmetry model, appropriate for the trigonal space group of $Ba_4Ni_{1.94}Ir_{2.06}O_{12}$, and populating the energy states with 14 electrons [4 electrons for each iridium(V) and 6 electrons for nickel(IV)] results in two unpaired electrons in the e_g^2 highest occupied molecular orbital, as shown in Figure 4.

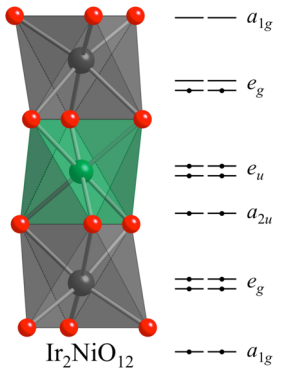

Figure 4. Schematic energy-level diagram of an Ir_2NiO_{12} trimer with local D_{3d} symmetry, approximated from $Ir_3^{4.33}O_{12}$ trimers with comparable D_{3d} symmetry.

Combining these two unpaired electrons with the two unpaired electrons in the $Ni^{II}O_6$ units results in a calculated magnetic moment of 3.94 μ_B, close to the measured moment of 4.40 μ_B. One could contemplate the formal oxidation states resulting from this arrangement; depending on which cation provides the final electrons, an oxidation state distribution of $Ir_2^{V}Ni^{IV}$ or $Ir_2^{IV}Ni^{VI}$ could be envisioned. On the basis of the XANES and XPS data, it seems clear that the former is a better description of the trimer's oxidation state distribution.

In summary, we have reported on the preparation and characterization of single crystals of the new iridium-containing quadruple perovskite, $Ba_4Ni_{1.94}Ir_{2.06}O_{12}$, with an unusual coexistence of nickel(II) and nickel(IV). The measured magnetic susceptibility was explained by the combined effect of a magnetic Ir_2NiO_{12} trimer and two unpaired electrons residing on the nickel(II) cation.

■ ASSOCIATED CONTENT

Supporting Information

The material is available free of charge via the Internet at The Supporting Information is available free of charge on the ACS Publications website at DOI: 10.1021/acs.inorgchem.8b00249.

Experimental setup, crystallographic structure information, XANES, XPS spectra, magnetic data plots and tables, PXRD patterns, SEM images, temperature dependence plots, and energy-splitting diagram (PDF)

Accession Codes

CCDC 1544900–1544901 contain the supplementary crystallographic data for this paper. These data can be obtained free of charge via www.ccdc.cam.ac.uk/data_request/cif, or by emailing data_request@ccdc.cam.ac.uk, or by contacting The Cambridge Crystallographic Data Centre, 12 Union Road, Cambridge CB2 1EZ, UK; fax: +44 1223 336033.

■ AUTHOR INFORMATION

Corresponding Author

*E-mail: zurloye@mailbox.sc.edu.

ORCID

Hans-Conrad zur Loye: 0000-0001-7351-9098

Notes

The authors declare no competing financial interest.

■ ACKNOWLEDGMENTS

This work was supported, in part, by a University of South Carolina ASPIRE II award and, in part, by the National Science Foundation under Awards DMR-1301757 and OIA-1655740. This research used resources of the APS, an Office of Science User Facility operated for the U.S. Department of Energy (DOE) Office of Science by ANL, and was supported by the U.S. DOE under Contract DE-AC02-06CH11357 and the Canadian Light Source and its funding partners.

■ REFERENCES

(1) Kim, Y. K.; Sung, N. H.; Denlinger, J. D.; Kim, B. J. Observation of a d-wave gap in electron-doped Sr_2IrO_4. *Nat. Phys.* **2016**, *12*, 37–41.

(2) Pesin, D.; Balents, L. Mott physics and band topology in materials with strong spin-orbit interaction. *Nat. Phys.* **2010**, *6*, 376–381.

(3) Okamoto, Y.; Nohara, M.; Aruga-Katori, H.; Takagi, H. Spin-Liquid State in the $S = {}^1/_2$ Hyperkagome Antiferromagnetic $Na_4Ir_3O_8$. *Phys. Rev. Lett.* **2007**, *99*, 137207.

(4) Haskel, D.; Fabbris, G.; Zhernenkov, M.; Kong, P. P.; Jin, C. Q.; Cao, G.; van Veenendaal, M. Pressure Tuning of the Spin-Orbit Coupled Ground State in Sr_2IrO_4. *Phys. Rev. Lett.* **2012**, *109*, 027204.

(5) Clancy, J. P.; Chen, N.; Kim, C. Y.; Chen, W. F.; Plumb, K. W.; Jeon, B. C.; Noh, T. W.; Kim, Y.-J. Spin-orbit coupling in iridium-based 5d compounds probed by x-ray absorption spectroscopy. *Phys. Rev. B: Condens. Matter Mater. Phys.* **2012**, *86*, 195131.

(6) Lupascu, A.; Clancy, J. P.; Gretarsson, H.; Nie, Z.; Nichols, J.; Terzic, J.; Cao, G.; Seo, S. S. A.; Islam, Z.; Upton, M. H.; Kim, J.; Casa, D.; Gog, T.; Said, A. H.; Katukuri, V. M.; Stoll, H.; Hozoi, L.; van den

DOI: 10.1021/acs.inorgchem.8b00249
Inorg. Chem. 2018, 57, 2973–2976

Brink, J.; Kim, Y.-J. Tuning Magnetic Coupling in Sr_2IrO_4 Thin Films with Epitaxial Strain. *Phys. Rev. Lett.* **2014**, *112*, 147201.
(7) Phelan, B. F.; Krizan, J.; Xie, W.; Gibson, Q.; Cava, R. J. New material for probing spin-orbit coupling in iridates. *Phys. Rev. B: Condens. Matter Mater. Phys.* **2015**, *91*, 155117.
(8) Rau, J. G.; Lee, E. K.-H.; Kee, H.-Y. Spin-Orbit Physics Giving Rise to Novel Phases in Correlated Systems: Iridates and Related Materials *Annu. Rev. Annu. Rev. Condens. Matter Phys.* **2016**, *7*, 195−211.
(9) Flynn, J.; Li, J.; Sleight, A. W.; Ramirez, A.; Subramanian, M. A. Structure and Properties of Ir-Containing Oxides with Large Spin-Orbit Coupling: $Ba_2In_{1-x}Ir_xO_{5+\delta}$. *Inorg. Chem.* **2016**, *55*, 2748−2754.
(10) Cuthbert, H. L.; Greedan, J. E.; Vargas-Baca, I.; Derakhshan, S.; Swainson, I. P. Synthesis, Structure, and Unexpected Magnetic Properties of $La_3Re_2O_{10}$. *Inorg. Chem.* **2007**, *46*, 8739−8745.
(11) Shimoda, Y.; Doi, Y.; Hinatsu, Y.; Ohoyama, K. Synthesis, Crystal Structures, and Magnetic Properties of New 12L-Perovskites Ba4LnRu3O12 (Ln = Lanthanides). *Chem. Mater.* **2008**, *20*, 4512−4518.
(12) Shimoda, Y.; Doi, Y.; Wakeshima, M.; Hinatsu, Y. Crystal Structures and Characterizations of Mixed Valence 12L-Perovskites $Ba_4EuM_3O_{12}$ (M = Ru and Ir). *Inorg. Chem.* **2009**, *48*, 9952−9957.
(13) Shimoda, Y.; Doi, Y.; Wakeshima, M.; Hinatsu, Y. Magnetic and electrical properties of quadruple perovskites with 12 layer structures $Ba_4LnM_3O_{12}$ (Ln = rare earths; M = Ru, Ir): The role of metal-metal bonding in perovskite-related oxides. *J. Solid State Chem.* **2010**, *183*, 1962−1969.
(14) Miiller, W.; Dunstan, M. T.; Huang, Z.; Mohamed, Z.; Kennedy, B. J.; Avdeev, M.; Ling, C. D. Complex 5d Magnetism in a Novel $S = {}^1/_2$ Trimer System, the 12L Hexagonal Perovskite $Ba_4BiIr_3O_{12}$. *Inorg. Chem.* **2013**, *52*, 12461−12467.
(15) Giaquinta, D. M.; zur Loye, H. C. Structural Predictions in the ABO_3 Phase Diagram. *Chem. Mater.* **1994**, *6*, 365−372.
(16) Macquart, R.; Kim, S.-J.; Gemmill, W. R.; Stalick, J. K.; Lee, Y.; Vogt, T.; zur Loye, H.-C. Synthesis, Structure and Magnetic Properties of Sr_2NiOsO_6 and Ca_2NiOsO_6: Two New Osmium Containing Double Perovskites. *Inorg. Chem.* **2005**, *44*, 9676−9683.
(17) Blum, C. G. F.; Holcombe, A.; Gellesch, M.; Sturza, M. I.; Rodan, S.; Morrow, R.; Maljuk, A.; Woodward, P.; Morris, P.; Wolter, A. U. B.; Buchner, B.; Wurmehl, S. Flux growth and characterization of Sr_2NiWO_6 single crystals. *J. Cryst. Growth* **2015**, *421*, 39−44.
(18) Mugavero, S. J., III; Fox, A. H.; Smith, M. D.; zur Loye, H. C. Crystal Growth, Structure and Magnetic Properties of the Double Perovskites Ln_2MgIrO_6 (Ln = Pr, Nd, Sm-Gd). *J. Solid State Chem.* **2010**, *183*, 465−470.
(19) zur Loye, H.-C.; Kim, S.-J.; Macquart, R.; Smith, M. D.; Lee, Y.; Vogt, T. Low temperature structural phase transition of $Ba_3NaIr_2O_9$. *Solid State Sci.* **2009**, *11*, 608−613.
(20) Mugavero, S. J., III; Smith, M. D.; Yoon, W.-S.; zur Loye, H.-C. $Nd_2K_2IrO_7$ and $Sm_2K_2IrO_7$: Iridium (VI) Oxides Prepared under Ambient Pressure. *Angew. Chem., Int. Ed.* **2009**, *48*, 215−218.
(21) Mugavero, S. J., III; Smith, M. D.; zur Loye, H. C. The crystal growth and magnetic properties of Ln_2LiIrO_6 (*Ln* = Pr, Nd, Sm, Eu). *J. Solid State Chem.* **2005**, *178*, 200−206.
(22) Mugavero, S. J., III; Smith, M. D.; zur Loye, H. C. $La_{2.50}K_{1.50}IrO_7$: An Example of an n = 2 Member of the $A_nB_{n-1}O_{3n}$ (A′2O) Family of Perovskite Related Oxides. *J. Solid State Chem.* **2005**, *178*, 3176−3182.
(23) Powell, A. V.; Gore, J. G.; Battle, P. D. The magnetic properties of iridium in mixed-metal oxides. *J. Alloys Compd.* **1993**, *201*, 73.
(24) Stitzer, K. E.; Smith, M. D.; Gemmill, W. R.; zur Loye, H. C. Novel Mixed-Valent (V/VI) Triple Perovskite Ruthenates: Observation of a Complex Low Temperature Structural and Magnetic Transition. *J. Am. Chem. Soc.* **2002**, *124*, 13877−13885.
(25) Lufaso, M. W.; Woodward, P. W. Predictions of the crystal structures of perovskites using the software program SPuDS. *Acta Crystallogr., Sect. B: Struct. Sci.* **2001**, *57*, 725−738.
(26) Laguna-Marco, M. A.; Kayser, P.; Alonso, J. A.; Martinez-Lope, M. J.; van Veenendaal, M.; Choi, Y.; Haskel, D. Electronic structure, local magnetism, and spin-orbit effects of Ir(IV)-,Ir(V)-,and Ir(VI)-based compounds. *Phys. Rev. B: Condens. Matter Mater. Phys.* **2015**, *91*, 214433.
(27) Ferreira, T.; Morrison, G.; Yeon, J.; zur Loye, H.-C. Design and Crystal Growth of Magnetic Double Perovskite Iridates: Ln_2MIrO_6 (*Ln* = La, Pr, Nd, Sm-Gd; M = Mg, Ni). *Cryst. Growth Des.* **2016**, *16*, 2795−2803.
(28) Seki, H.; Hosaka, Y.; Saito, T.; Mizumaki, M.; Shimakawa, Y. Ferromagnetism Induced by Substitution of the Iron(IV) Ion by an Unusual High-Valence Nickel (IV) Ion in Antiferromagnetic $SrFeO_3$. *Angew. Chem., Int. Ed.* **2016**, *55*, 1360−1363.

DOI: 10.1021/acs.inorgchem.8b00249
Inorg. Chem. 2018, 57, 2973−2976